PERGAMON

International Journal of Heat and Mass Transfer 42 (1999) 4363–4374

International Journal of HEAT and MASS TRANSFER

www.elsevier.com/locate/ijhmt

Measurements and theoretical modelling of the effective thermal conductivity of zeolites

A. Griesinger, K. Spindler, E. Hahne*

Institut für Thermodynamik und Wärmetechnik, Universität Stuttgart, Pfaffenwaldring 6, D-70550 Stuttgart, Germany

Received 17 November 1998; received in revised form 25 February 1999

Abstract

The use of zeolites as an adsorbent for water or ammonia in heat pumps and cooling systems is an interesting alternative to the traditional refrigerants. Recently, zeolites are also in discussion as hydrogen storage material. For all these applications the effective thermal conductivity of the zeolites is an important thermophysical property. The effective thermal conductivity λ_{eff} was measured by using the transient hot-wire method with an accuracy of ± 5–15%. The accuracy increases with increasing effective thermal conductivity. Hydrogen, argon, helium, nitrogen and air were used as filling gas. The gas pressure was varied in the range of 1 mbar $\leq p \leq$ 30 bar and the temperature in the range of 210 K $\leq T \leq$ 570 K. A simple model is proposed to calculate the effective thermal conductivity of the zeolite powder with an accuracy of about $\pm 30\%$.

1. Introduction

Since a few years zeolites are used as adsorbent in heat pumps and cooling systems. Recently, zeolites are also in discussion as hydrogen storage materials. The hydrogen molecules are forced into the zeolitic cages under pressure (30 bar) and high temperature (600 K). After cooling down and depressurization the hydrogen remains encased in the intercristalline cavities. Decapsulation of the trapped hydrogen molecules can be achieved by heating the loaded zeolite. The desorption of hydrogen from zeolites as well as the adsorption requires a heat supply [1,2]. The effective thermal conductivity λ_{eff} of the zeolite powders strongly influences the velocity of adsorbing and desorbing of hydrogen. For both applications, the use of zeolites as adsorbent in heat pumps and cooling systems and as hydrogen storage material the effective thermal conductivity and the specific heat are important thermophysical properties. Measurements of the specific heat are given in an earlier work [3].

2. Experimental apparatus and procedure

The measuring principle of the transient hot-wire method is based on the calculation of the transient temperature field around a thin wire which is heated with a constant current [4]. The wire is surrounded by the sample, whose thermal conductivity is to be measured. The current is switched on at time $t = 0$ s. The heat dissipated in the wire causes a temperature rise in the wire and in the sample. The temperature rise in the wire depends on the thermal conductivity of the sample. For an ideal continuous line source in an infinite homogeneous and isotropic medium the temperature rise for large values of t is given by Carslaw and Jaeger [5].

* Corresponding author. Tel.: +49-711-685-3536; fax: +49-711-685-3503.

E-mail address: pm@itw.uni-stuttgart.de (E. Hahne)

0017-9310/99/$ - see front matter
PII: S0017-9310(99)00096-4

Nomenclature

a (m^2/s)	thermal diffusivity
C_A (m)	gas specific constant in Eq. (6)
C_B (K)	gas specific constant in Eq. (6)
d (mm, μm)	particle size
k	gas specific parameter
Kn	Knudsen number
l (mm)	length of the heating wire
l_{fl} (m)	mean free path of the gas molecules
$\Delta L = 1$ m	unit length of the resistance model
p (bar)	pressure
$p_o = 0.0133$ (bar)	reference pressure
$\dot{q}_l$ (W/m)	heat dissipated per unit length of the line source
r (m)	distance from the heating wire
t (s)	time
T (K)	absolute temperature
ΔT (K)	temperature rise of the heating wire
T_o (K)	initial temperature of the heating wire
V_{net} (ml)	net volume of the measuring cell.

Greek symbols

α_p	fit parameter
δ (μm)	mean diameter of the pores
ϵ	emissivity
ϕ (mm)	diameter of the heating wire
γ	accommodation coefficient
κ	adiabatic exponent
λ, λ_{eff} (W/m K)	thermal conductivity, effective thermal conductivity
λ_o (W/m K)	thermal conductivity of the filling gas at $p = 1$ bar
$\lambda_{1,2,3}$ (W/m K)	thermal conductivity of path 1, 2 and 3
λ_{fl} (W/m K)	pressure dependent thermal conductivity of the fluid
$\lambda'_{fl} = \lambda_{fl} + \lambda_{rad}$ (W/m K)	total thermal conductivity of the gas phase
λ_{rad} (W/m K)	thermal conductivity by radiation
λ_s (W/m K)	thermal conductivity of the pure solid material
ν ($\ln(\nu) = 0.5772$)	Euler constant
ρ (kg/m^3)	density
$\sigma = 5.67051$ (W/m^2 K^4)	Stefan–Boltzmann constant
ψ	porosity.

$$\Delta T = T - T_o = \frac{\dot{q}_l}{4\pi\lambda} \ln\left(\frac{4at}{r^2\nu}\right) \tag{1}$$

(ΔT is the temperature rise at a radius r from the line source after a certain time t, T_o is the initial temperature, $\dot{q}_l$ is the dissipated heat per unit length of the line source, a is the thermal diffusivity and ν is the Euler constant ($\ln(\nu) = 0.5772$)). By differentiation of Eq. (1) with respect to $\ln(t)$ the thermal conductivity λ can be calculated

$$\lambda = \frac{\dot{q}_l}{4\pi} \Big/ \frac{\mathrm{d}(\Delta T)}{\mathrm{d}(\ln(t))}. \tag{2}$$

The platinum wire ($\phi = 0.2$ mm, length $l = 117$ mm) is used simultaneously for heating and as a resistance thermometer. The values of $\mathrm{d}(\Delta T)/\mathrm{d}(\ln(t))$ are obtained by measuring the voltage change of the heating wire, which is caused by the temperature dependent resistance change. The measuring cell, a stainless steel tube of $V_{net} = 217$ ml (Fig. 1), is contained in a pressure chamber. The steel tube contains the zeolite powder together with the heating wire and its support. The tube is closed at both ends with porous steel plates for gas inlet and outlet. The pressure chamber is temperature controlled up to 650 K. It is designed for a pressure range of 0.01 mbar $\leq p \leq$ 50 bar. More details about the apparatus are given by Kallweit [6].

3. Specifications of the zeolites

The zeolite type, the product name, the state of material as supplied, the particle size, the porosity and the density of the zeolites are listed in Table 1. The grain size distribution was measured with a laser-optical method. It shows almost a Gaussian-distribution. In Table 1 the mean diameter of the particles is given. The porosity of the zeolites was measured by filling up the powder with water. It can be calculated by:

$$\psi = \frac{V_{zeo} - V_{sludge} + V_{H_2O}}{V_{zeo}} \tag{3}$$

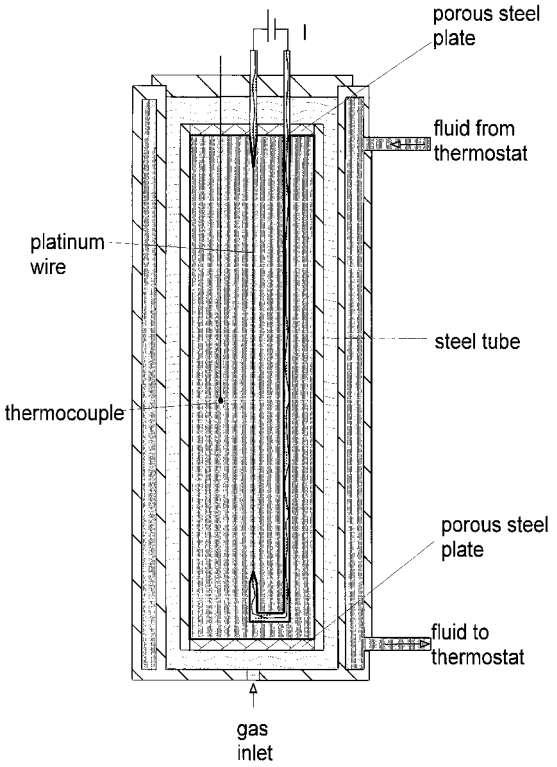

Fig. 1. Schematic diagram of the measuring cell.

(V_{zeo} is the volume of the dehydrated zeolite powder, V_{H_2O} is the volume of the water and V_{sludge} is the volume of the zeolite sludge, which is obtained by filling up the powder with water). For dehydration, the zeolites were heated up to 600 K at 1 mbar pressure. For hydration they were spread out for two weeks at 300 K and an air humidity of 50%. The density of the zeolite powder refers to the completely hydrated zeolites.

4. Results

4.1. The influence of temperature

The effective thermal conductivity of zeolite KA was measured in the temperature range of 210 K $\leq T \leq$ 570 K under atmospheric pressure (Fig. 2). At the beginning of the measurements at 210 K the zeolite was completely hydrated. The measurements were carried out with increasing temperature. For comparison the thermal conductivity of air at 1 bar is also shown in Fig. 2. A linear regression of the measured effective thermal conductivity of zeolite KA yields:

$$\lambda_{eff} = 0.023775\,\mathrm{W/m\,K} + (0.00014\,\mathrm{W/m\,K^2})T \qquad (4)$$

The maximum deviation between the measured effective thermal conductivity and the regression line is $\pm 3\%$.

4.2. The influence of pressure and filling gas

The curves of λ_{eff} depending on the pressure show a typical S-shape, see Fig. 3. For elevated pressures ($p \geq 10$ bar) see Fig. 3 there is almost no dependence of λ_{eff} on pressure. At these pressure, λ_{eff} is distinctly affected by the thermal conductivity of the filling gas: the effective thermal conductivity of the zeolite powder increases with increasing thermal conductivity of the filling gas. At a pressure of 10 bar, the effective thermal conductivity of zeolite NaA filled with hydrogen is 6 times higher than with argon (the thermal conductivity of hydrogen is at 473 K about 12 times higher than the thermal conductivity of argon). With decreasing pressure the mean free path of the filling gas molecules increases and therefore λ_{eff} decreases (Smoluchowski effect). For low pressures ($p \approx 0.001$ bar) the heat transport in the zeolite powder is dominated by heat conduction in the pure solid material.

Table 1
Specifications of the zeolites

Zeolite type	Product name	Producer	Particle size	Porosity	Density
KA	Köstrolith 3A	[a]	3.03 μm (powder)	0.65	691 kg/m^3
NaA	Köstrolith 4A	[a]	4.31 μm (powder)	0.65	691 kg/m^3
CaA	Köstrolith 5A	[a]	7.37 μm (powder)	0.65	691 kg/m^3
KA	562	[b]	3.88 mm (spheres)	0.68	691 kg/m^3
NaY	R 20 A 1216	[c]	8.47 μm (powder)	0.65	691 kg/m^3
Sodalite	SOD-1	[d]	6.18 μm (powder)	0.65	691 kg/m^3

[a] Chemiewerk Bad Köstritz GmbH.
[b] Grace GmbH.
[c] Bayer AG.
[d] Institut für Technische Chemie I, Universität Stuttgart.

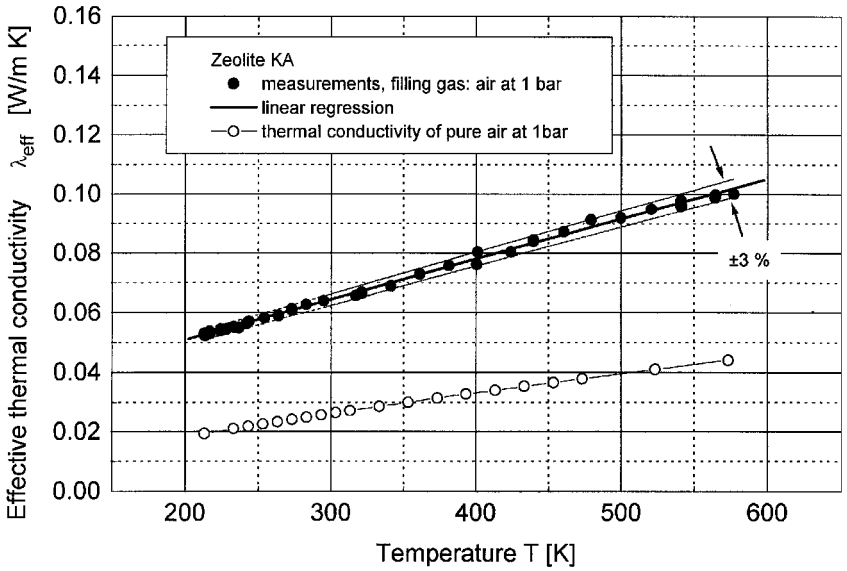

Fig. 2. Temperature dependence of the effective thermal conductivity of zeolite KA at atmospheric pressure.

Consequently there is only a small influence of the filling gas, except for hydrogen.

4.3. The effective thermal conductivity of different zeolites

Fig. 4 shows a comparison of the effective thermal conductivity of zeolite KA, NaA, Sodalite, CaA and NaY in the completely dehydrated state. Zeolite KA was measured as powder and as spheres. The effective thermal conductivity follows the particle size of the zeolites. Zeolite KA in spheres with the largest particle size (d = 3.88 mm) gives the highest effective thermal conductivity, zeolite KA in the powdery state with the smallest particle size (d = 3.0 μm) shows the lowest effective thermal conductivity. With increasing particle size the mean size of pores in the zeolite bed increases. For the zeolite spheres the mean free path of the hydrogen molecules is less than 1/100,000 of the mean size of a pore. The thermal conductivity of the filling

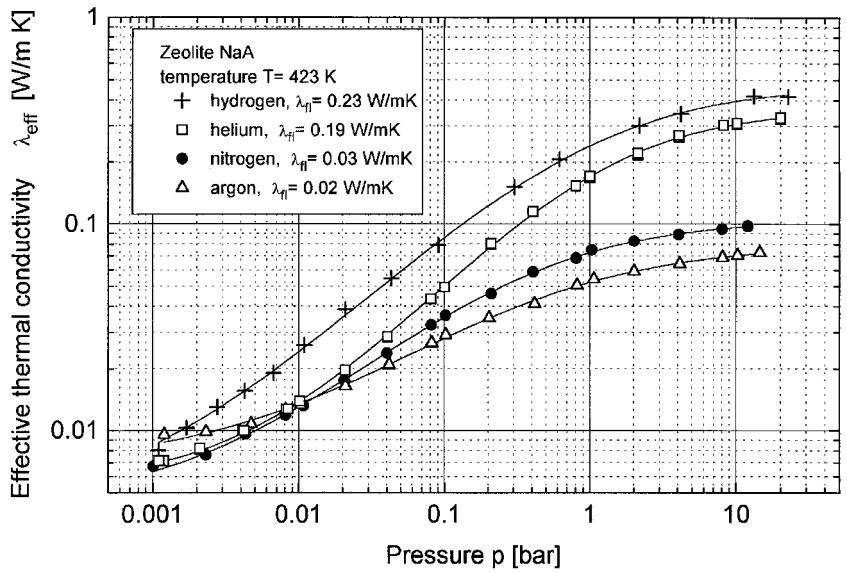

Fig. 3. Effective thermal conductivity of zeolite NaA with filling gas hydrogen, helium, nitrogen and argon.

gas is therefore nearly independent on the pressure. The effective thermal conductivity of the zeolite spheres does not decrease with decreasing pressure, see Fig. 4.

An investigation by Sahnoune and Grenier [7] with NaX pellets ($d = 4$ mm) in a helium atmosphere showed values in the range of $\lambda_{eff} = 0.03$–0.213 W/m K.

4.4. The influence of the adsorbed water on the effective thermal conductivity

The effective thermal conductivity of zeolite KA was measured in the completely hydrated state and in the completely dehydrated state, see Fig. 5. The filling gas was hydrogen. For high pressures ($p \geq 1$ bar) the water molecules encased in the cavities of the zeolite improve the effective thermal conductivity of the zeolite powder up to 30%.

4.5. The influence of the number of storing cycles on the effective thermal conductivity

For practical applications the cycle stability is an important requirement for the reversible encapsulation and decapsulation of the gas molecules in the zeolite. The effective thermal conductivity of zeolite NaA was measured during 50 storing cycles, see Fig. 6. For each storing cycle, λ_{eff} of the unloaded zeolite at 3 mbar/565 K and of the loaded zeolite at 1 bar/315 K was measured. The effective thermal conductivity did not change. Deviations are within the experimental scatter. Fig. 7 shows the particle size distribution of zeolite NaA before and after 50 storing cycles. There is no systematic change in the particle size distribution. The average diameter of the particles changes from $d = 4.31$ μm to $d = 4.23$ μm after 50 storing cycles. This difference of 2% is within the measurement error. The zeolite particles did not decompose after encapsulation of hydrogen molecules in the cavities of the zeolite.

4.6. The influence of graphite powder on the effective thermal conductivity

The effective thermal conductivity of zeolite powders varies between 0.007 W/m K at 1 mbar and 0.41 W/m K at 30 bar, see Fig. 3. These low values of the effective thermal conductivity require high temperature gradients to heat up the zeolites. Efforts have been made to improve the effective thermal conductivity of the zeolites by mixing the zeolite powder with graphite powder with an effective thermal conductivity of 0.88 W/m K (under normal conditions). The graphite powder consists of laminas with an average diameter of 347 μm. Fig. 8 shows the effective thermal conductivity of zeolite KA and the mixture with 10, 20 and 30% by weight of graphite powder. The density of the pure zeolite powder and the powder mixtures is kept constant to $\rho = 691$ kg/m^3. For pressures $p \geq 0.1$ bar the effective thermal conductivity of the zeolite powder is increased by a factor of 4 for a 30% share of graphite powder. For lower pressures ($p < 0.01$ bar) the influence of the graphite powder is smaller. With increasing

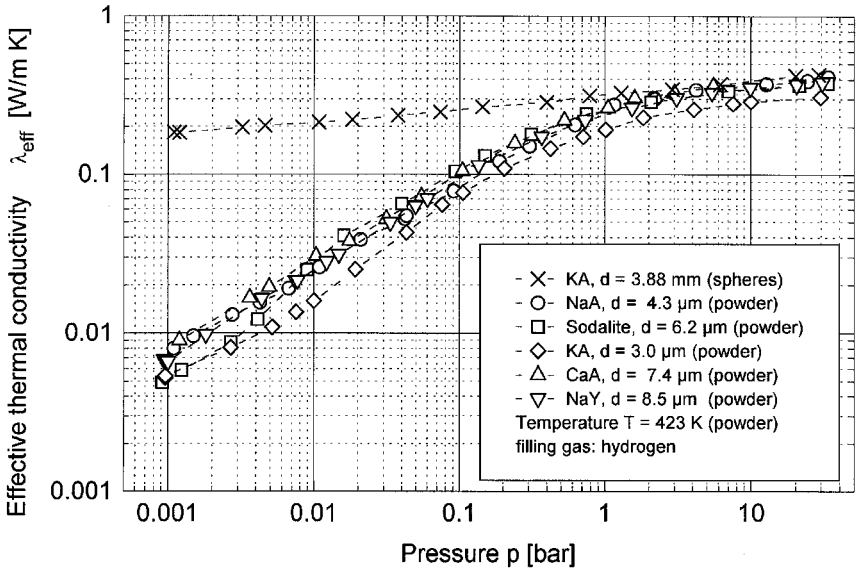

Fig. 4. Effective thermal conductivity of zeolite powders and pellets (spheres).

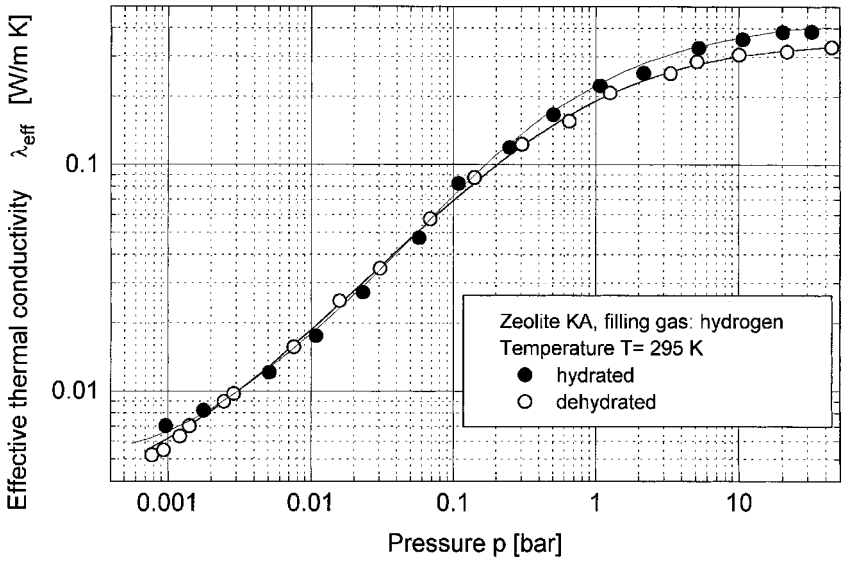

Fig. 5. Effective thermal conductivity of zeolite NaA in the hydrated and in the dehydrated state.

percentage of the graphite powder the porosity of the powder mixture increases as the density of the mixture is kept constant and the density of a graphite particle is bigger than the density of a zeolite particle. With increasing porosity of the mixture the effective thermal conductivity decreases. With decreasing pressure this effect gets more important, because with decreasing pressure the effective thermal conductivity is more and more influenced by the heat conduction in the pure solid material.

5. Theoretical modelling

The effective thermal conductivity of a packed bed is influenced by primary and secondary parameters [8]. Primary parameters are the thermal conductivities of the two phases (particles, gas) and the porosity of the system. Secondary parameters describe the heat transfer by radiation, the shape of the particles and the grain size distribution, the mean diameter of the pores, the pressure dependence of the thermal conductivity of

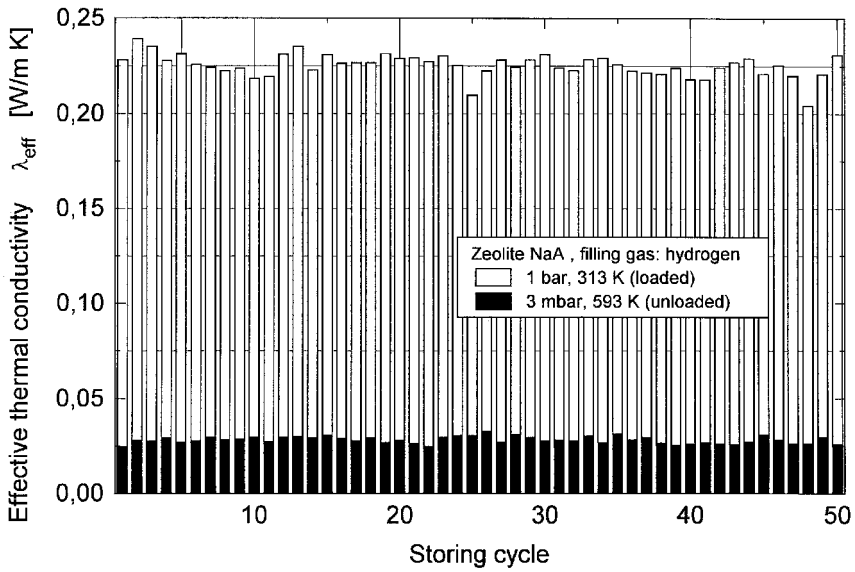

Fig. 6. Effective thermal conductivity of zeolite NaA in the loaded and in the unloaded state.

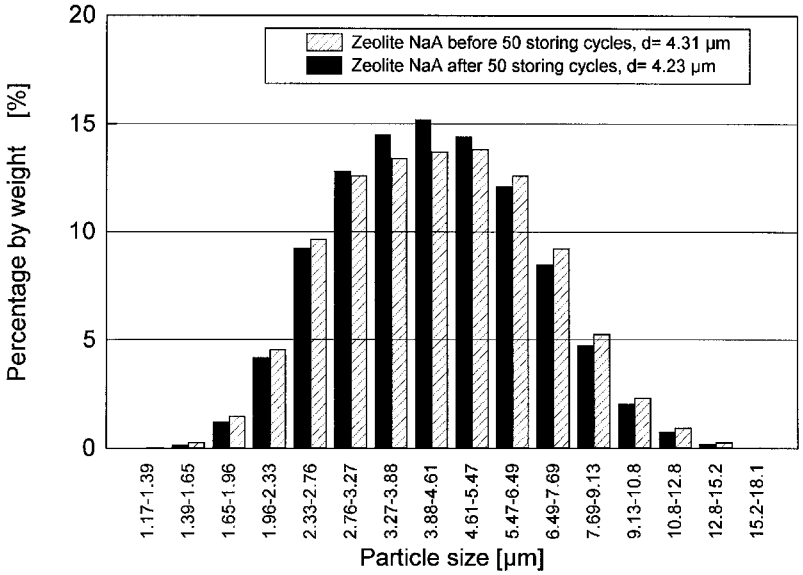

Fig. 7. Particle size distribution before and after 50 storing cycles.

the filling gas and the flattening of the particles caused by a mechanical pressure. Some of these primary and secondary parameters are known or can be measured directly like the thermal conductivity of the gas, the porosity, optical properties of the packed bed, the shape of the particles or the grain size distribution. Other parameters cannot be measured directly with a sufficient accuracy. These parameters are the thermal conductivity of the solid material (in the case of small particles) and the flattening of the particles due to a mechanical pressure. These parameters can only be determined by experiment. For this the calculated values of the effective thermal conductivity based on the model are fitted to the measured values.

All models concerning the effective thermal conductivity of packed beds can be classified in three types. In the models of type one the packed bed is represented by a unit cell. The temperature field in this

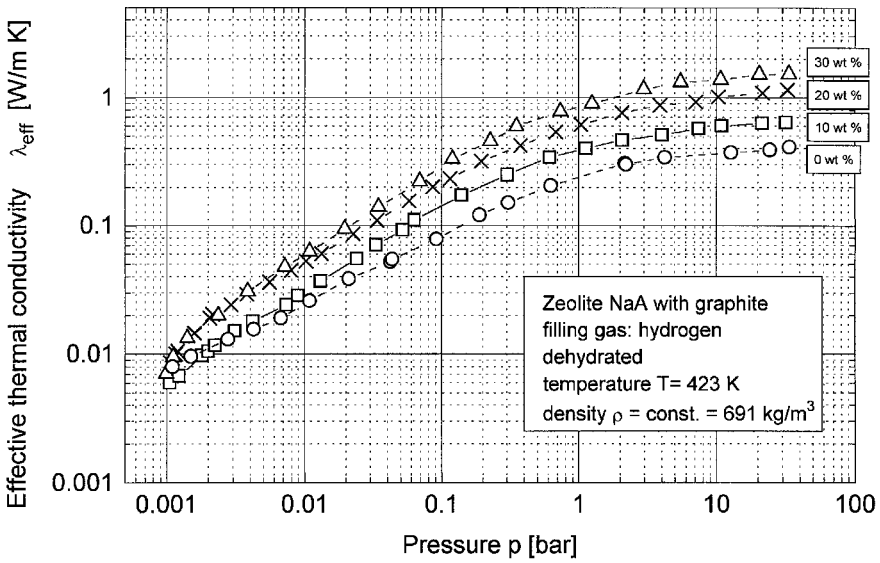

Fig. 8. Effective thermal conductivity of zeolite NaA with 0, 10, 20 and 30 wt% graphite.

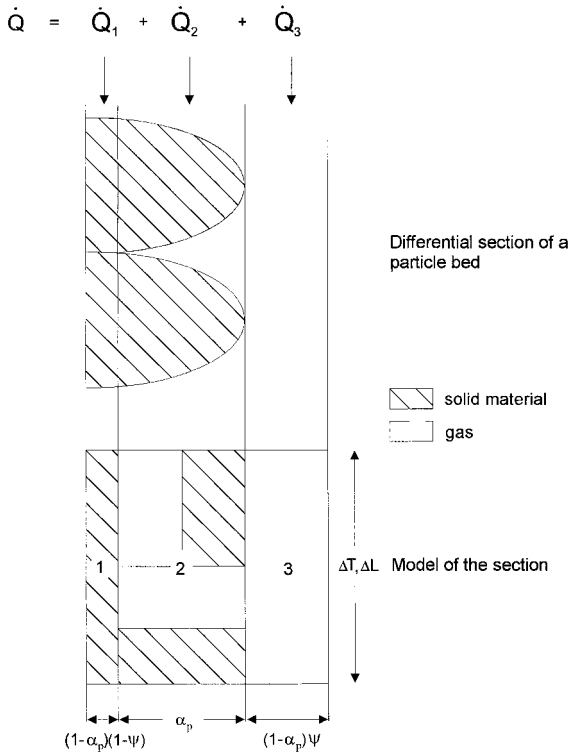

Fig. 9. Resistance model for the effective thermal conductivity of zeolite powders.

unit cell is calculated. From the temperature distribution the heat flux and the effective thermal conductivity of the probe can be obtained. In the models of type two the packed bed is represented by a unit cell, too. The effective thermal conductivity of this unit cell is calculated by assuming various simplifications. In the models of type three the porous system is replaced by a combination of thermal resistances which are connected in parallel and in series.

The effective thermal conductivity of zeolite powders can be described by a simple model of type two, see Fig. 9. In analogy to the model by Zehner, Bauer and Schlünder [9–11] the heat transport is subdivided into three paths with different relative areas: a pure solid path (1), a mixed path with a solid and a fluid part (2), and a pure fluid path (3). The parameter α_p describes the relative area of the mixed path of the unit cell. The relative area of the pure fluid path is $(1-\alpha_p)\psi$, the relative area of the pure solid path is $(1-\alpha_p)(1-\psi)$, see Fig. 9. The thermal conductivity of the filling gas λ_{fl} is given by Kaganer [12] as

$$\lambda_{fl} = \frac{\lambda_o}{1 + 2\beta Kn} \tag{5}$$

where λ_o is the thermal conductivity of the filling gas at $p = 1$ bar, $\beta = 2k(2-\gamma)/(\gamma(\kappa+1))$, with k being the gas specific parameter and $Kn = l_{fl}/\delta$ the Knudsen number. The accommodation coefficient γ describes the effectiveness of energy transfer between the gas molecules and the solid material. The mean free path of the molecules l_{fl} is given by Sutherland [13] with

$$l_{fl} = \frac{p_o C_A}{p(1 + C_B/T)}. \tag{6}$$

C_A and C_B are gas specific constants. The heat trans-

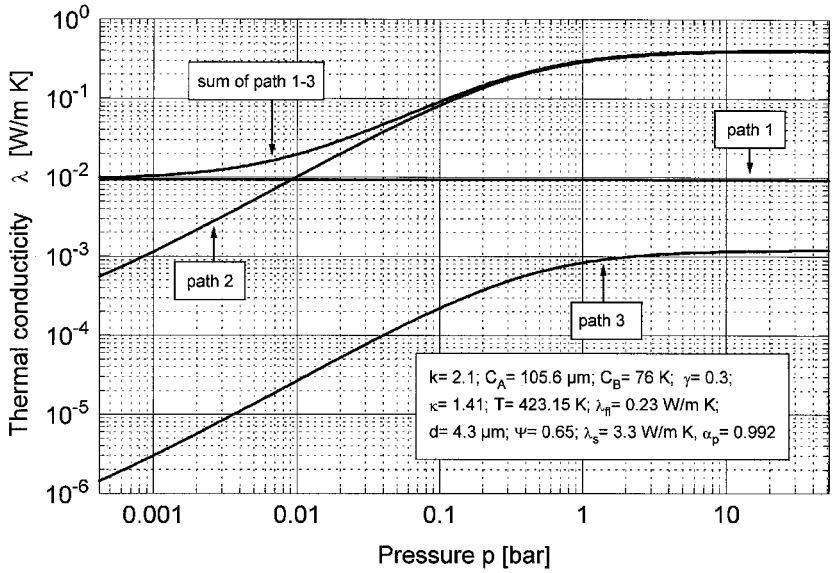

Fig. 10. Thermal conductivity of path 1, 2 and 3 of the resistance model. Calculated for zeolite KA with filling gas hydrogen.

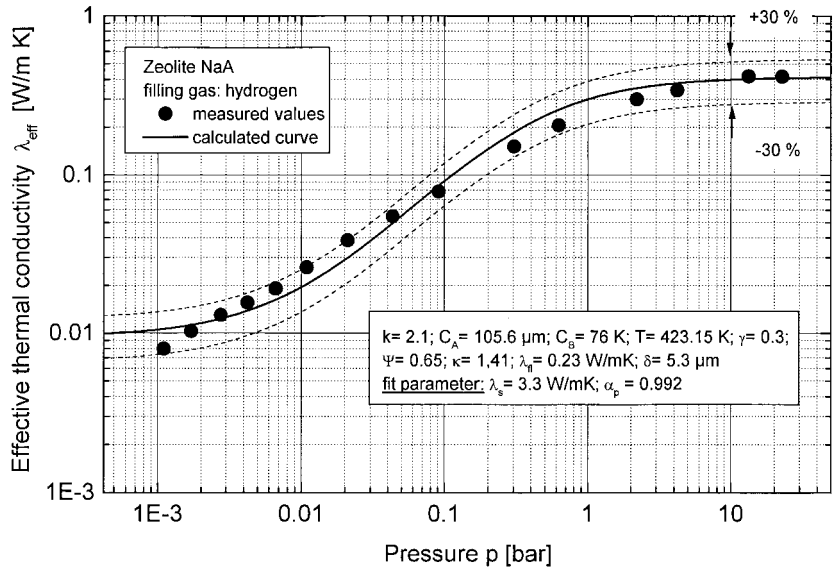

Fig. 11. Comparison of the measured and calculated effective thermal conductivity of zeolite NaA with filling gas hydrogen.

port by radiation is taken into account by

$$\lambda_{\mathrm{rad}} = \frac{4\sigma T^3 d}{2/\epsilon - 1} \tag{7}$$

as given by Damköhler [14]. Thus the thermal conductivity in the gas phase becomes $\lambda'_{\mathrm{fl}} = \lambda_{\mathrm{fl}} + \lambda_{\mathrm{rad}}$.

Assuming a one directional (e.g. vertical) heat flow, the total heat flow of the unit cell is given by:

$$\dot{Q} = \dot{Q}_1 + \dot{Q}_2 + \dot{Q}_3. \tag{8}$$

With the relative areas of the three paths and the total area of the unit cell $A = 1\ \mathrm{m}^2$, Eq. 8 changes to [15]:

$$\dot{q} = (1-\alpha_{\mathrm{p}})(1-\psi)\dot{q}_1 + \alpha_{\mathrm{p}}\dot{q}_2 + (1-\alpha_{\mathrm{p}})\psi\dot{q}_3 \tag{9}$$

$$\dot{q} = [(1-\alpha_{\mathrm{p}})(1-\psi)\lambda_1] + \alpha_{\mathrm{p}}\lambda_2 + (1-\alpha_{\mathrm{p}})\psi\lambda_3]\frac{\Delta T}{\Delta L} \tag{10}$$

$$\dot{q} = \lambda_{\mathrm{eff}}\frac{\Delta T}{\Delta L} \tag{11}$$

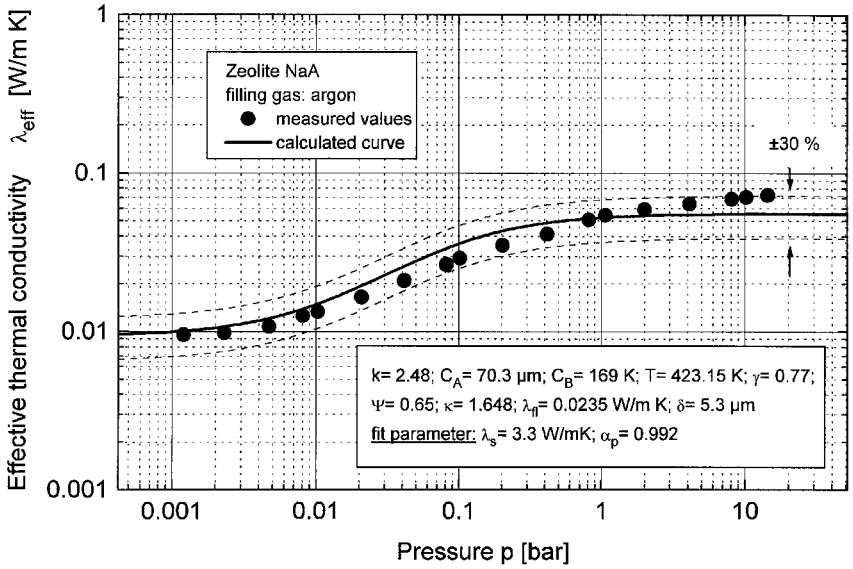

Fig. 12. Comparison of the measured and calculated effective thermal conductivity of zeolite NaA with filling gas argon.

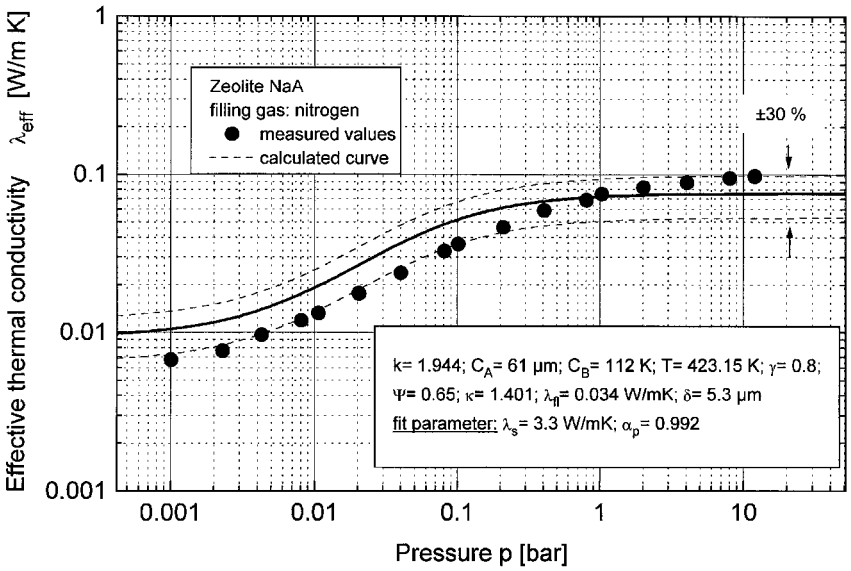

Fig. 13. Comparison of the measured and calculated effective thermal conductivity of zeolite NaA with filling gas nitrogen.

with

$$\lambda_{\mathrm{eff}} = (1-\alpha_{\mathrm{p}})(1-\psi)\lambda_{\mathrm{s}} + \frac{2\alpha_{\mathrm{p}}}{1/(\lambda'_{\mathrm{fl}}+\lambda_{\mathrm{s}}) + 1/\lambda'_{\mathrm{fl}} + 1/\lambda_{\mathrm{s}}} + (1-\alpha_{\mathrm{p}})\psi\lambda'_{\mathrm{fl}}. \quad (12)$$

The values of C_{A}, C_{B}, γ, k, κ and λ_{fl} are given in [8]. The emissivity ϵ of the zeolite powders was measured with an infrared camera. For all zeolites the emissivity is $\epsilon = 0.89$. Fig. 10 shows the thermal conductivity of path 1, 2 and 3 calculated for zeolite KA with the filling gas hydrogen. The thermal conductivity of path 3 (pure fluid path) has only a small influence on the effective thermal conductivity. For pressures $p \leq 0.01$ bar the effective thermal conductivity is strongly influ-

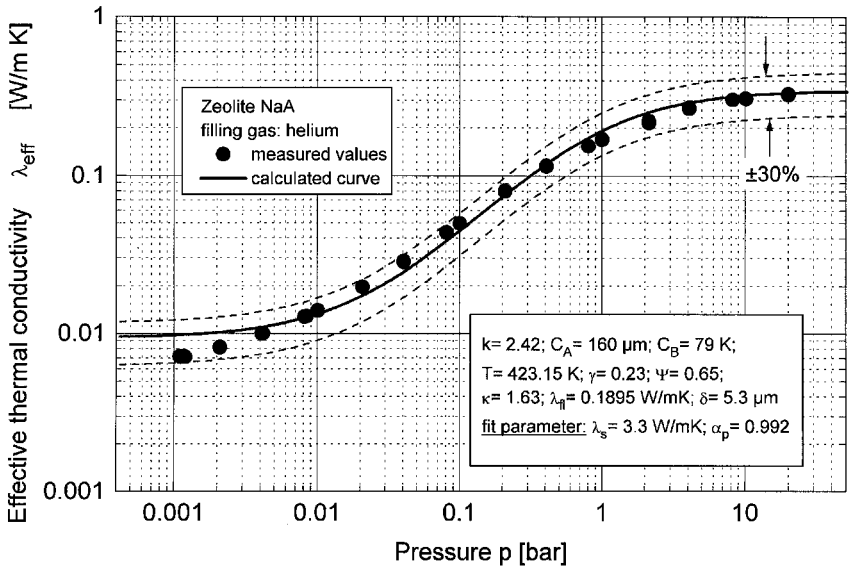

Fig. 14. Comparison of the measured and calculated effective thermal conductivity of zeolite NaA with filling gas helium.

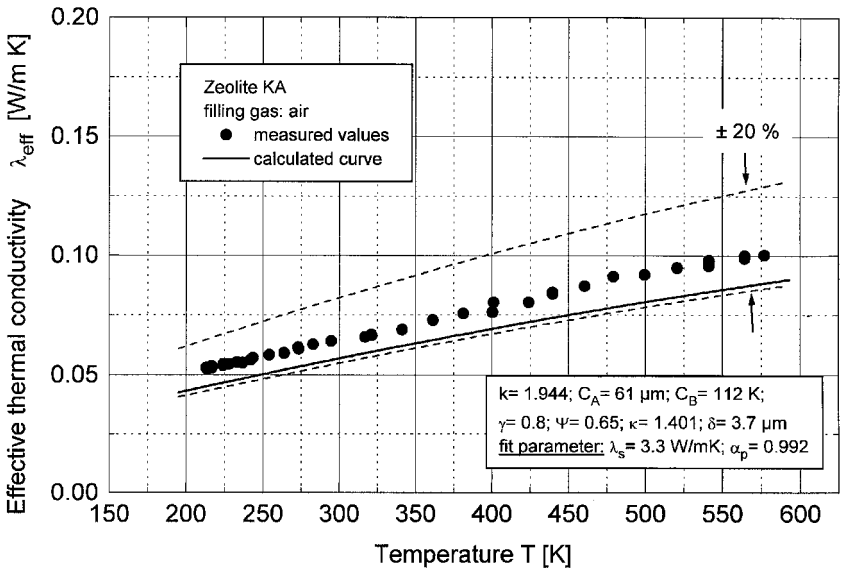

Fig. 15. Comparison of the calculated and measured temperature dependence of the effective thermal conductivity of zeolite KA.

enced by the thermal conductivity of path 1 (pure solid path). For higher pressures $p \geq 0.01$ bar the effective thermal conductivity is dominated by the thermal conductivity of path 2.

The thermal conductivity of the pure zeolite λ_s and the fit parameter α_p has to be determined by fitting the theoretical curve (Eq. 12) to the measured values. Fitting the theoretical curve to measured values in the pressure range of 1 mbar $\leq p \leq$ 30 bar and the temperature range of 210 K $\leq T \leq$ 570 K result in $\lambda_s = 3.3$ W/m K. The fit parameter is found to be $\alpha_p = 0.992$. The effective thermal conductivity of zeolite powders can be calculated with an accuracy of about $\pm 30\%$. Figs. 11–14 give a comparison of the measured and calculated effective thermal conductivity of zeolite NaA with the filling gases hydrogen, argon, nitrogen and helium at 423 K. The mean deviation of the calculated values from the measured values is 16.5%. The temperature dependence of the effective thermal conductivity of zeolite KA at 1 bar pressure is described by this resistance model within an accuracy of about $\pm 20\%$, as shown in Fig. 15.

The influence of pressure and temperature on the effective thermal conductivity is well described by the model without changing the fit parameter α_p.

Acknowledgement

This work was supported by 'Deutsche Forschungsgemeinschaft' through 'Sonderforschungsbereich 270: Energieträger Wasserstoff'. The authors gratefully acknowledge this support.

References

[1] D. Fraenkel, R. Lazar, J. Shabtai, The potential of zeolite molecular sieves as hydrogen storage media, Alternative Energy Sources 8 (1977) 3771–3802.
[2] J. Weitkamp, M. Fritz, S. Ernst, Zeolithe als Speichermaterialen für Wasserstoff, Chem.-Ing.-Tech. 64 (1992) 1106–1109.
[3] A. Griesinger, K. Spindler, E. Hahne, Zeolite powders as hydrogen storage materials: measurements and theoretical modelling of thermophysical properties, Hydrogen Energy Progress XI, in: Proceedings of the Eleventh Hydrogen Energy Conference, Stuttgart, 1996, 3, pp. 2513–2522.
[4] J.J. Healy, J.J. de Groot, J. Kerstin, The theory of the transient hot-wire method for measuring thermal conductivity, Physica 82C (1976) 392–408.
[5] H.S. Carsalw, J.C. Jaeger, Conduction of Heat in Solids, Oxford University Press, London, 1959.
[6] J. Kallweit, Effektive Wärmeleitfähigkeit von Metallhydrid-Materialien zur Speicherrung von Wasserstoff, Dissertation, Universität Stuttgart, 1994.
[7] H. Sahnoune, Ph Grenier, Mesure de la conductivité thermique d'une zéolite, The Chemical Engineering Journal 42 (1989) 45–54.
[8] VDI-Wärmeatlas, Chapter Dee: Wämeleitfähigkeit von Schüttschichten, 7, erweiterte Auflage, VDI-Verlag, Düsseldorf, 1994.
[9] P. Zehner, E.U. Schlünder, Wärmeleitfähigkeit von Schüttungen bei mässigen Temperaturen, Chem.-Ing.-Techn. 42 (14) (1970) 933–941.
[10] P. Zehner, E.U. Schlünder, Einfluss der Wärmestrahlung und des Druckes auf den Wärmetransport in nicht durchströmten Schüttungen, Chem.-Ing.-Techn. 44 (23) (1972) 1303–1308.
[11] R. Bauer, E.U. Schlünder, Effective radial thermal con-

ductivity of packings in gas flow, Part II, Thermal conductivity of the packing fraction without gas flow, Int. Chem. Eng. 18 (2) (1978) 189–204.

[12] M.G. Kaganer, Thermal Insulation in Cryogenic Engineering, Engl. translation by A. Moscana, Israel Progr. Sci. Transl., Jerusalem, 1969, von Teplovaya Izolyatsiya v Tekhnike Nizkikh Temperatur, Izdatel'stvo 'Mashinostroenie', Moskau, 1966.

[13] W. Sutherland, The viscosity of gases and molecular force, Phil. Mag. 36 (1893) 507–531.

[14] G. Damköhler, Einfluss von Diffusion, Strömung und Wärmetransport auf die Ausbeute bei chemisch-technischen Reaktionen, A. Eucken, M. Jakob, (Hrsg.), Akad. Verlagsges., 3, Leipzig, 1937.

[15] A. Griesinger, Experimentelle und theoretische Untersuchung des Wärmetransports in Zeolithschüttungen, Dissertation, Universität Stuttgart, 1998.